371/2011

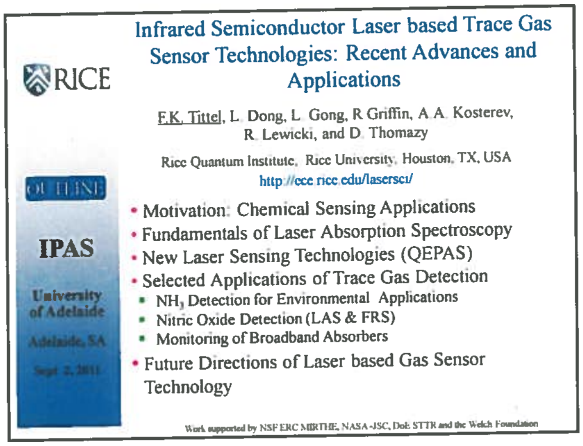

Infrared Semiconductor Laser based Trace Gas Sensor Technologies: Recent Advances and Applications

F.K. Tittel, L. Dong, L. Gong, R Griffin, A A. Kosterev, R. Lewicki, and D. Thomazy

Rice Quantum Institute, Rice University, Houston, TX, USA
http://ece.rice.edu/lasersci/

OUTLINE

IPAS
University of Adelaide
Adelaide, SA
Sept 2, 2011

- Motivation: Chemical Sensing Applications
- Fundamentals of Laser Absorption Spectroscopy
- New Laser Sensing Technologies (QEPAS)
- Selected Applications of Trace Gas Detection
  - NH_3 Detection for Environmental Applications
  - Nitric Oxide Detection (LAS & FRS)
  - Monitoring of Broadband Absorbers
- Future Directions of Laser based Gas Sensor Technology

Work supported by NSF ERC MIRTHE, NASA-JSC, DoE STTR and the Welch Foundation

Rice University, Houston

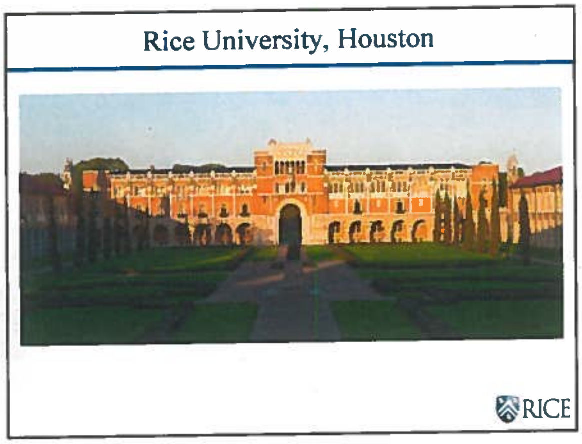

Rice University, Houston

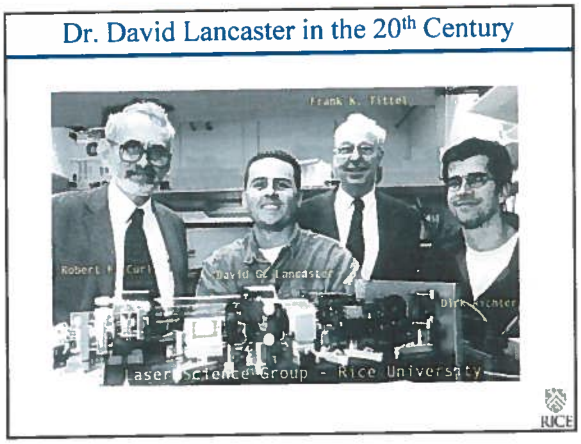

Dr. David Lancaster in the 20th Century

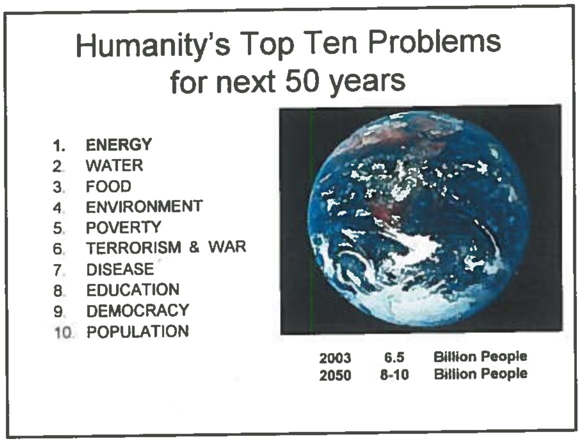

Humanity's Top Ten Problems for next 50 years

1. ENERGY
2. WATER
3. FOOD
4. ENVIRONMENT
5. POVERTY
6. TERRORISM & WAR
7. DISEASE
8. EDUCATION
9. DEMOCRACY
10. POPULATION

2003	6.5	Billion People
2050	8-10	Billion People

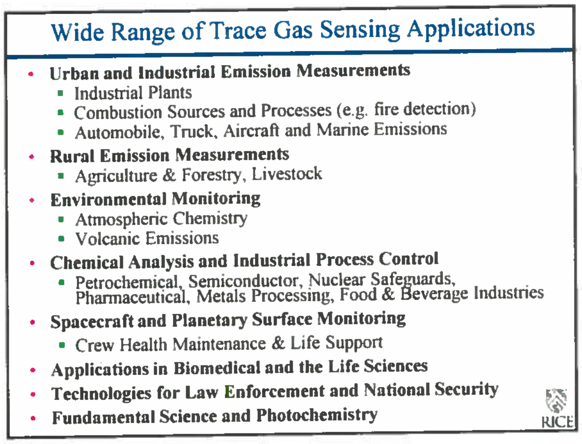

Wide Range of Trace Gas Sensing Applications

- **Urban and Industrial Emission Measurements**
  - Industrial Plants
  - Combustion Sources and Processes (e.g. fire detection)
  - Automobile, Truck, Aircraft and Marine Emissions
- **Rural Emission Measurements**
  - Agriculture & Forestry, Livestock
- **Environmental Monitoring**
  - Atmospheric Chemistry
  - Volcanic Emissions
- **Chemical Analysis and Industrial Process Control**
  - Petrochemical, Semiconductor, Nuclear Safeguards, Pharmaceutical, Metals Processing, Food & Beverage Industries
- **Spacecraft and Planetary Surface Monitoring**
  - Crew Health Maintenance & Life Support
- **Applications in Biomedical and the Life Sciences**
- **Technologies for Law Enforcement and National Security**
- **Fundamental Science and Photochemistry**

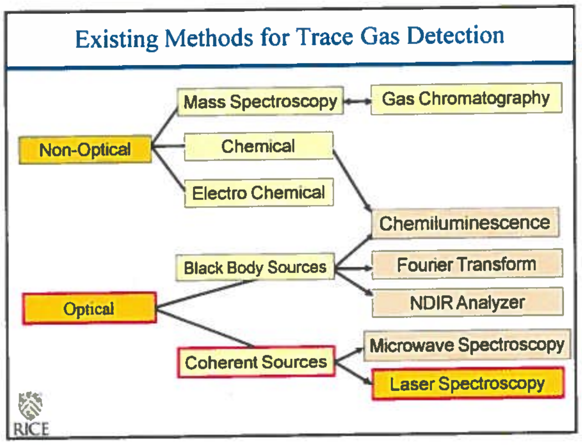

Existing Methods for Trace Gas Detection

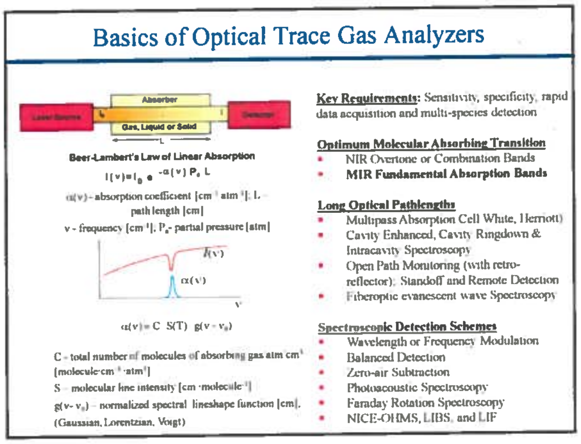

Basics of Optical Trace Gas Analyzers

Beer-Lambert's Law of Linear Absorption

$I(\nu) = I_0\, e^{-\alpha(\nu)\, P_a\, L}$

$\alpha(\nu)$ - absorption coefficient [$cm^{-1}\, atm^{-1}$]; L - path length [cm]

ν - frequency [cm^{-1}]; P_a - partial pressure [atm]

$\alpha(\nu) = C \cdot S(T) \cdot g(\nu - \nu_0)$

C - total number of molecules of absorbing gas atm cm^{-1} [molecule cm^{-3} atm^{-1}]

S - molecular line intensity [cm molecule^{-1}]

$g(\nu - \nu_0)$ - normalized spectral lineshape function [cm], (Gaussian, Lorentzian, Voigt)

Key Requirements: Sensitivity, specificity, rapid data acquisition and multi-species detection

Optimum Molecular Absorbing Transition
- NIR Overtone or Combination Bands
- **MIR Fundamental Absorption Bands**

Long Optical Pathlengths
- Multipass Absorption Cell White, Herriott)
- Cavity Enhanced, Cavity Ringdown & Intracavity Spectroscopy
- Open Path Monitoring (with retro-reflector); Standoff and Remote Detection
- Fiberoptic evanescent wave Spectroscopy

Spectroscopic Detection Schemes
- Wavelength or Frequency Modulation
- Balanced Detection
- Zero-air Subtraction
- Photoacoustic Spectroscopy
- Faraday Rotation Spectroscopy
- NICE-OHMS, LIBS, and LIF

7

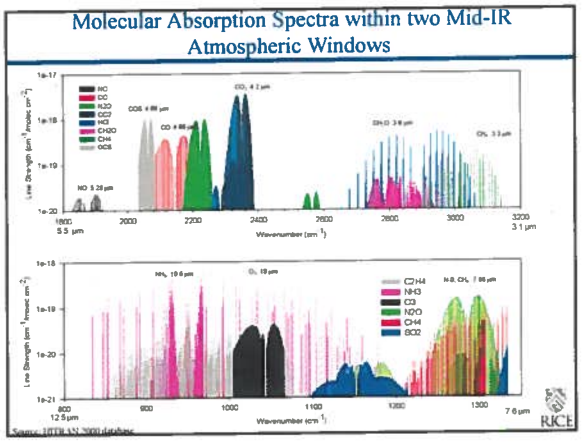

Molecular Absorption Spectra within two Mid-IR Atmospheric Windows

Source: HITRAN 2000 database

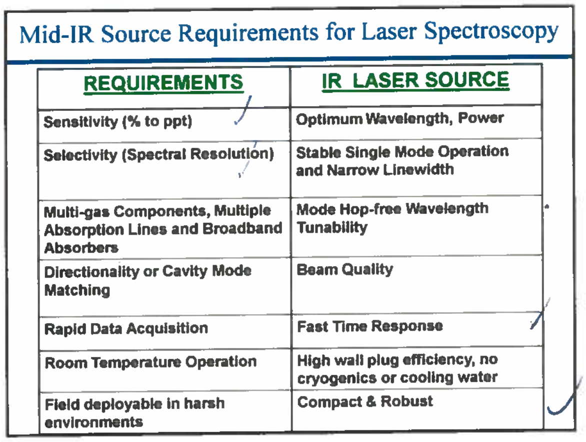

Mid-IR Source Requirements for Laser Spectroscopy

REQUIREMENTS	IR LASER SOURCE
Sensitivity (% to ppt)	Optimum Wavelength, Power
Selectivity (Spectral Resolution)	Stable Single Mode Operation and Narrow Linewidth
Multi-gas Components, Multiple Absorption Lines and Broadband Absorbers	Mode Hop-free Wavelength Tunability
Directionality or Cavity Mode Matching	Beam Quality
Rapid Data Acquisition	Fast Time Response
Room Temperature Operation	High wall plug efficiency, no cryogenics or cooling water
Field deployable in harsh environments	Compact & Robust

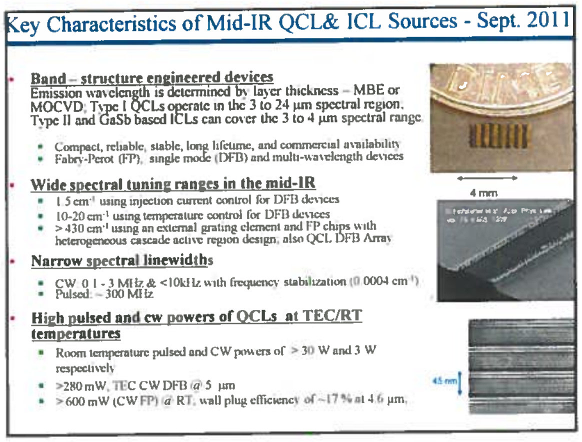

Key Characteristics of Mid-IR QCL& ICL Sources - Sept. 2011

- **Band – structure engineered devices**
  Emission wavelength is determined by layer thickness – MBE or MOCVD; Type I QCLs operate in the 3 to 24 µm spectral region. Type II and GaSb based ICLs can cover the 3 to 4 µm spectral range
  - Compact, reliable, stable, long lifetime, and commercial availability
  - Fabry-Perot (FP), single mode (DFB) and multi-wavelength devices
- **Wide spectral tuning ranges in the mid-IR**
  - 1.5 cm^{-1} using injection current control for DFB devices
  - 10-20 cm^{-1} using temperature control for DFB devices
  - > 430 cm^{-1} using an external grating element and FP chips with heterogeneous cascade active region design; also QCL DFB Array
- **Narrow spectral linewidths**
  - CW: 0.1 - 3 MHz & <10kHz with frequency stabilization (0.0004 cm^{-1})
  - Pulsed: ~ 300 MHz
- **High pulsed and cw powers of QCLs at TEC/RT temperatures**
  - Room temperature pulsed and CW powers of > 30 W and 3 W respectively
  - >280 mW, TEC CW DFB @ 5 µm
  - > 600 mW (CW FP) @ RT, wall plug efficiency of ~17 % at 4.6 µm,

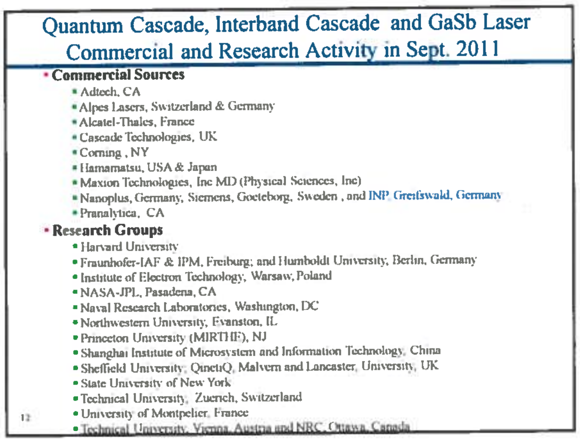

Quantum Cascade, Interband Cascade and GaSb Laser Commercial and Research Activity in Sept. 2011

- **Commercial Sources**
  - Adtech, CA
  - Alpes Lasers, Switzerland & Germany
  - Alcatel-Thales, France
  - Cascade Technologies, UK
  - Corning , NY
  - Hamamatsu, USA & Japan
  - Maxion Technologies, Inc MD (Physical Sciences, Inc)
  - Nanoplus, Germany, Siemens, Goeteborg, Sweden , and INP Greifswald, Germany
  - Pranalytica, CA
- **Research Groups**
  - Harvard University
  - Fraunhofer-IAF & IPM, Freiburg; and Humboldt University, Berlin, Germany
  - Institute of Electron Technology, Warsaw, Poland
  - NASA-JPL, Pasadena, CA
  - Naval Research Laboratories, Washington, DC
  - Northwestern University, Evanston, IL
  - Princeton University (MIRTHE), NJ
  - Shanghai Institute of Microsystem and Information Technology, China
  - Sheffield University, QinetiQ, Malvern and Lancaster, University, UK
  - State University of New York
  - Technical University, Zuerich, Switzerland
  - University of Montpelier, France
  - Technical University, Vienna, Austria and NRC, Ottawa, Canada

12

12

Widely Tunable, CW, TEC Quantum Cascade Lasers

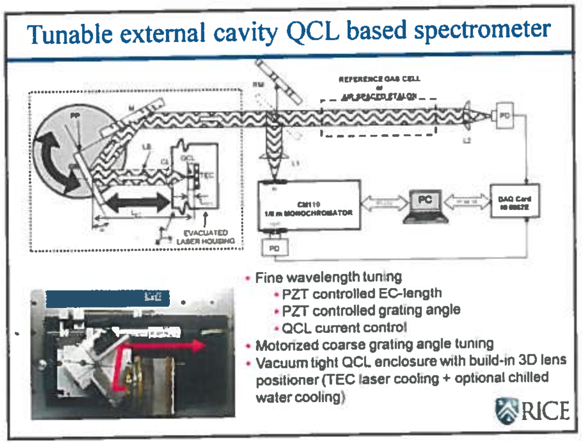

Tunable external cavity QCL based spectrometer

- Fine wavelength tuning
  - PZT controlled EC-length
  - PZT controlled grating angle
  - QCL current control
- Motorized coarse grating angle tuning
- Vacuum tight QCL enclosure with build-in 3D lens positioner (TEC laser cooling + optional chilled water cooling)

RICE

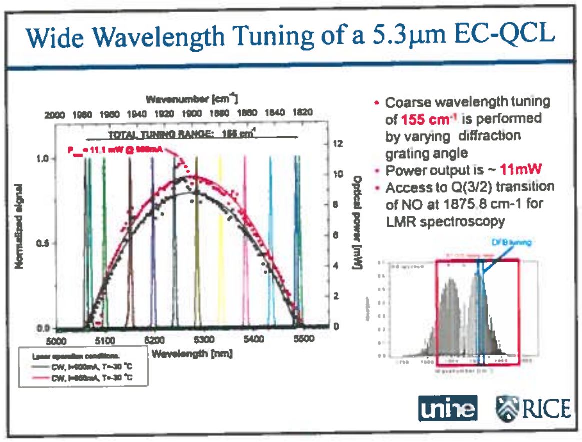

Wide Wavelength Tuning of a 5.3μm EC-QCL

- Coarse wavelength tuning of **155 cm⁻¹** is performed by varying diffraction grating angle
- Power output is ~ **11mW**
- Access to Q(3/2) transition of NO at 1875.8 cm-1 for LMR spectroscopy

unine RICE

Traditional and Quartz Enhanced Photoacoustic Spectroscopy

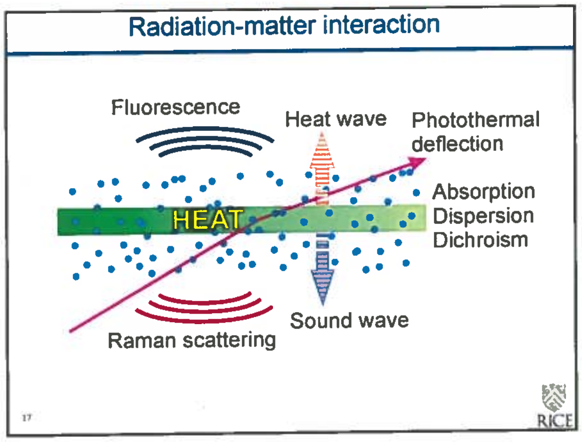

Radiation-matter interaction

Fluorescence

Heat wave

Photothermal deflection

HEAT

- Absorption
- Dispersion
- Dichroism

Sound wave

Raman scattering

RICE

✓

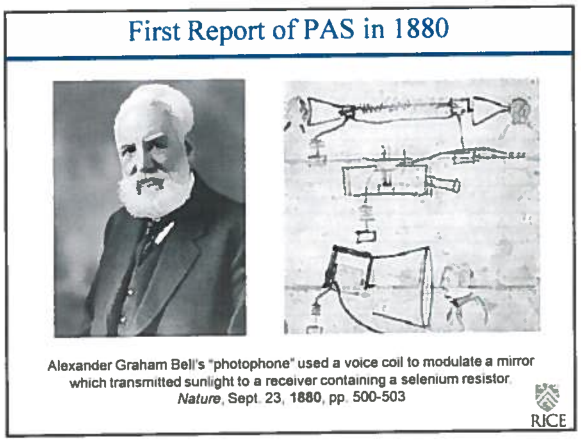

First Report of PAS in 1880

Alexander Graham Bell's "photophone" used a voice coil to modulate a mirror which transmitted sunlight to a receiver containing a selenium resistor. *Nature*, Sept. 23, 1880, pp. 500-503

RICE

18

From conventional PAS to QEPAS

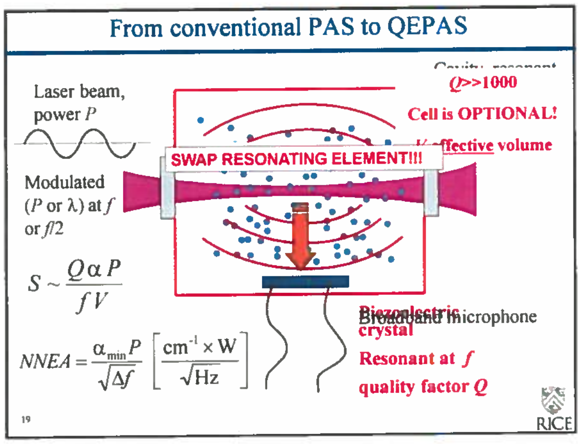

Q>>1000

Cell is OPTIONAL!

V – effective volume

$$S \sim \frac{Q \alpha P}{f V}$$

$$NNEA = \frac{\alpha_{\min} P}{\sqrt{\Delta f}} \left[\frac{\mathrm{cm}^{-1} \times \mathrm{W}}{\sqrt{\mathrm{Hz}}} \right]$$

Resonant at f

quality factor Q

Quartz Tuning Fork as a Resonant Microphone

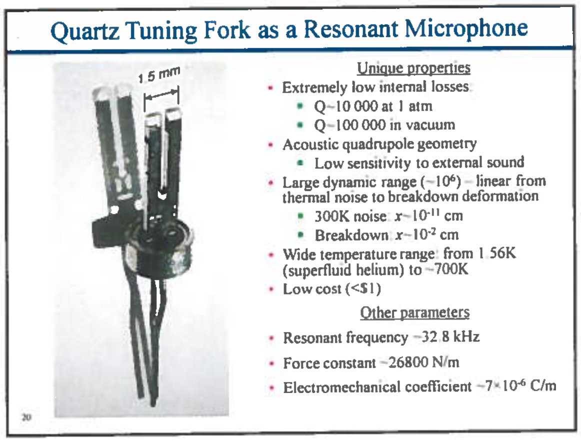

Unique properties

- Extremely low internal losses:
  - Q~10 000 at 1 atm
  - Q~100 000 in vacuum
- Acoustic quadrupole geometry
  - Low sensitivity to external sound
- Large dynamic range (~10^6) – linear from thermal noise to breakdown deformation
  - 300K noise: x~10^{-11} cm
  - Breakdown: x~10^{-2} cm
- Wide temperature range: from 1.56K (superfluid helium) to ~700K
- Low cost (<$1)

Other parameters

- Resonant frequency ~32.8 kHz
- Force constant ~26800 N/m
- Electromechanical coefficient ~7×10^{-6} C/m

Equivalent electrical circuit of a quartz tuning fork (QTF)

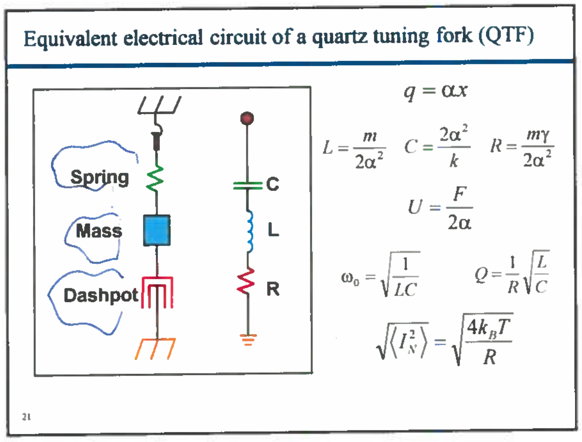

$$q = \alpha x$$

$$L = \frac{m}{2\alpha^2} \quad C = \frac{2\alpha^2}{k} \quad R = \frac{m\gamma}{2\alpha^2}$$

$$U = \frac{F}{2\alpha}$$

$$\omega_0 = \sqrt{\frac{1}{LC}} \qquad Q = \frac{1}{R}\sqrt{\frac{L}{C}}$$

$$\sqrt{\langle I_N^2 \rangle} = \sqrt{\frac{4k_B T}{R}}$$

QEPAS Spectrophone: QTF and Micro-resonator

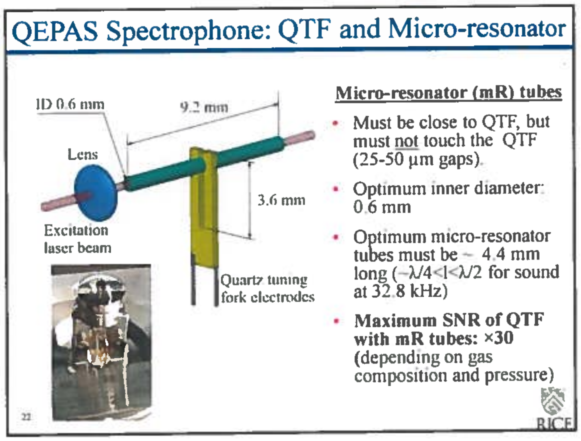

Micro-resonator (mR) tubes

- Must be close to QTF, but must not touch the QTF (25-50 µm gaps).
- Optimum inner diameter: 0.6 mm
- Optimum micro-resonator tubes must be ~ 4.4 mm long (~λ/4<l<λ/2 for sound at 32.8 kHz)
- **Maximum SNR of QTF with mR tubes: ×30** (depending on gas composition and pressure)

Alignment-free QEPAS Absorption Detection Module

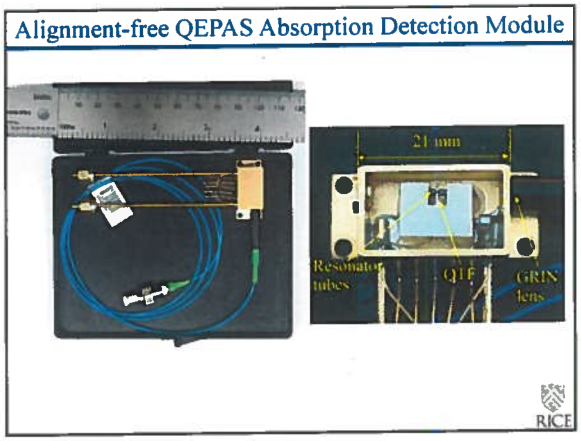

Off-beam QEPAS based Gas Sensor

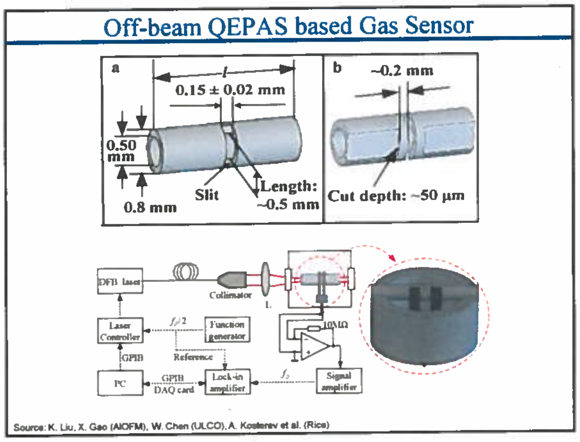

Source: K. Liu, X. Gao (AIOFM), W. Chen (ULCO), A. Kosterev et al. (Rice)

24

Tuning fork enhanced interferometric photoacoustic spectroscopy (TIPAS) based sensor

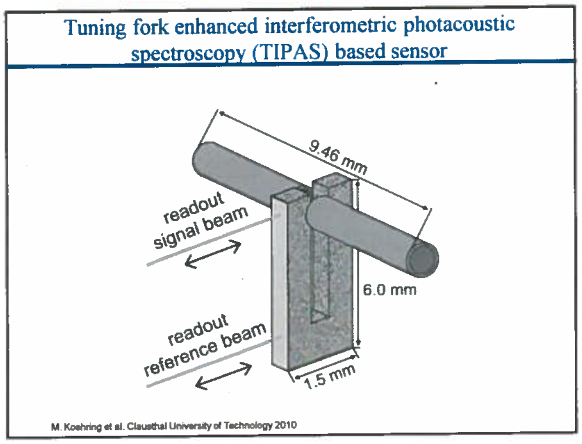

M. Koehring et al. Clausthal University of Technology 2010

~~QEPAS based sensor design for a can packaged λ=2.33 µm laser~~

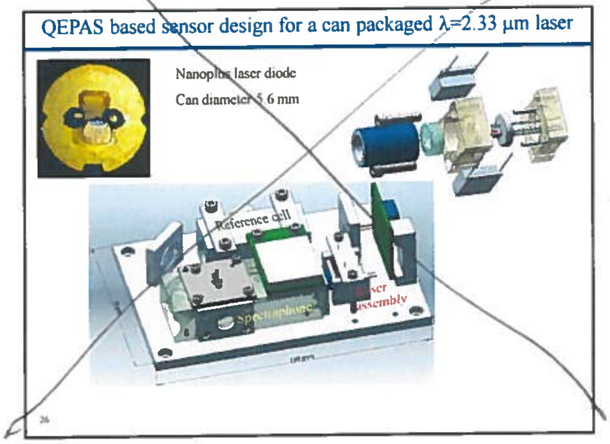

~~Nanoplus laser diode~~

~~Can diameter 5.6 mm~~

Principal Architecture of a QEPAS Gas Sensor

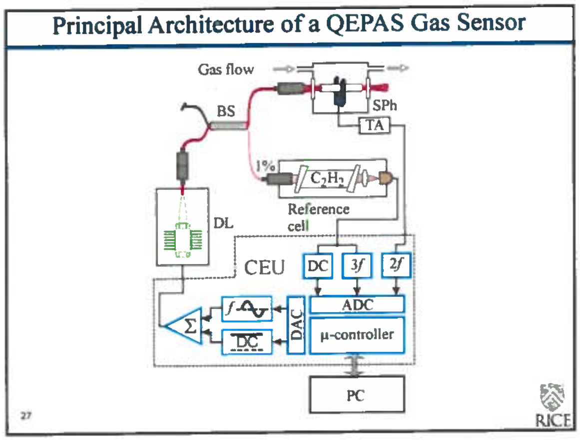

Typical QTF Resonance Curves

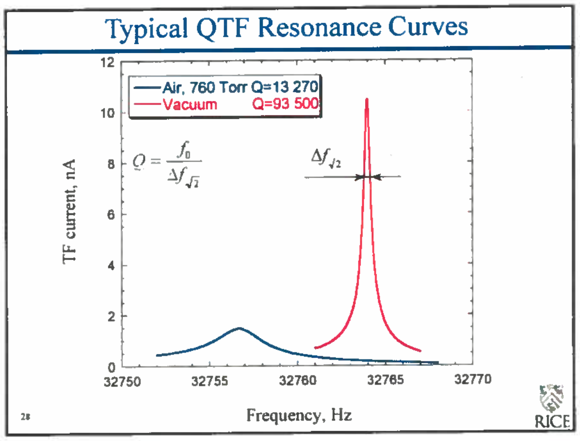

$$Q = \frac{f_0}{\Delta f_{\sqrt{2}}}$$

Signal-to-noise ratio as a function of pressures

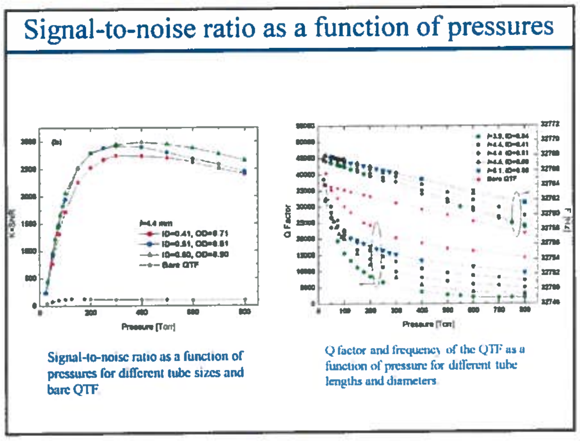

Signal-to-noise ratio as a function of pressures for different tube sizes and bare QTF

Q factor and frequency of the QTF as a function of pressure for different tube lengths and diameters

Acoustic and quartz resonators - interaction

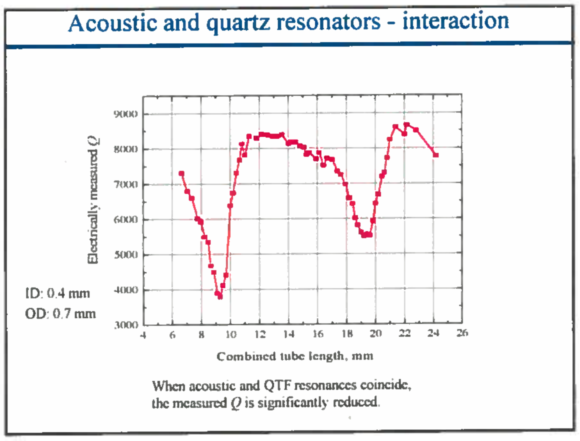

ID: 0.4 mm
OD: 0.7 mm

When acoustic and QTF resonances coincide, the measured Q is significantly reduced.

30

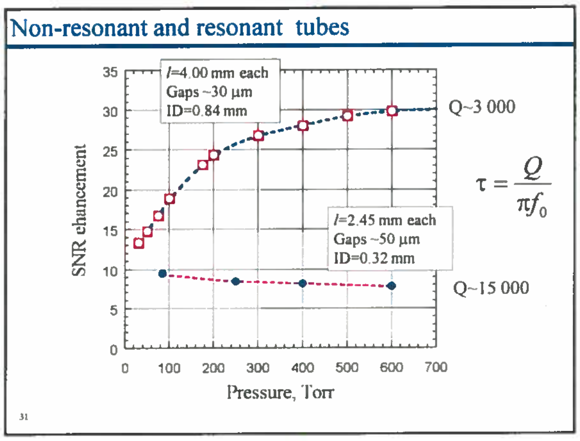

Non-resonant and resonant tubes

$$\tau = \frac{Q}{\pi f_0}$$

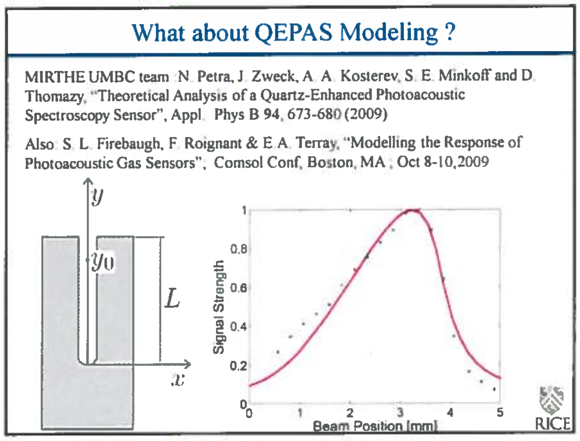

What about QEPAS Modeling ?

MIRTHE UMBC team: N. Petra, J. Zweck, A. A. Kosterev, S. E. Minkoff and D. Thomazy, "Theoretical Analysis of a Quartz-Enhanced Photoacoustic Spectroscopy Sensor", Appl. Phys B 94, 673-680 (2009)

Also S. L. Firebaugh, F. Roignant & E.A. Terray, "Modelling the Response of Photoacoustic Gas Sensors", Comsol Conf, Boston, MA, Oct 8-10,2009

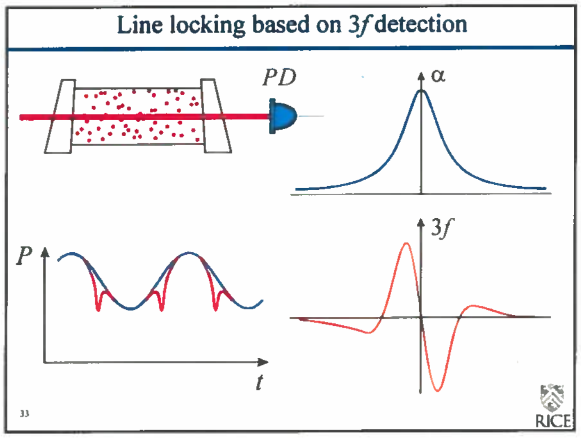

Line locking based on $3f$ detection

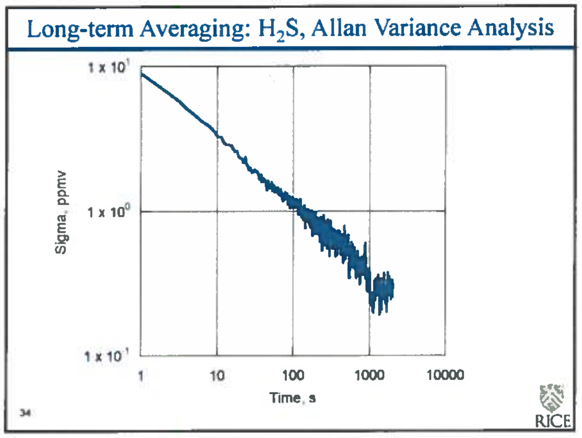

Long-term Averaging: H_2S, Allan Variance Analysis

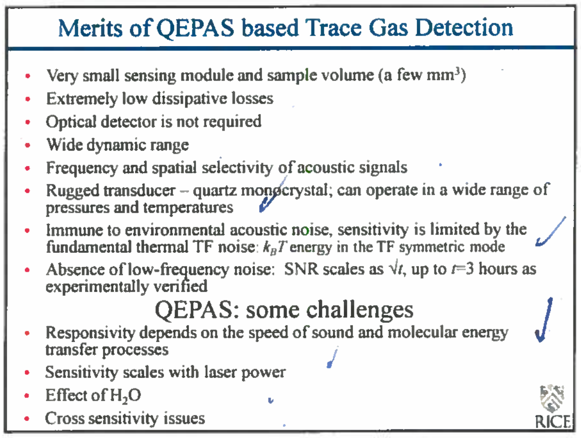

Merits of QEPAS based Trace Gas Detection

- Very small sensing module and sample volume (a few mm^3)
- Extremely low dissipative losses
- Optical detector is not required
- Wide dynamic range
- Frequency and spatial selectivity of acoustic signals
- Rugged transducer – quartz monocrystal; can operate in a wide range of pressures and temperatures
- Immune to environmental acoustic noise, sensitivity is limited by the fundamental thermal TF noise: k_BT energy in the TF symmetric mode
- Absence of low-frequency noise: SNR scales as $\sqrt{t}$, up to t=3 hours as experimentally verified

QEPAS: some challenges

- Responsivity depends on the speed of sound and molecular energy transfer processes
- Sensitivity scales with laser power
- Effect of H_2O
- Cross sensitivity issues

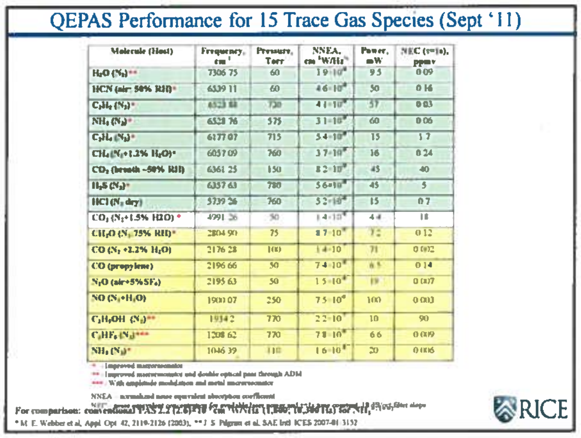

QEPAS Performance for 15 Trace Gas Species (Sept '11)

Molecule (Host)	Frequency, cm^{-1}	Pressure, Torr	NNEA, $cm^{-1}W/Hz^{1/2}$	Power, mW	NEC (τ=1s), ppmv
H_2O (N_2)**	7306.75	60	$1.9 \cdot 10^{-9}$	9.5	0.09
HCN (air: 50% RH)*	6539.11	60	$4.6 \cdot 10^{-9}$	50	0.16
C_2H_2 (N_2)*	6523.88	720	$4.1 \cdot 10^{-9}$	57	0.03
NH_3 (N_2)*	6528.76	575	$3.1 \cdot 10^{-9}$	60	0.06
C_2H_4 (N_2)*	6177.07	715	$5.4 \cdot 10^{-9}$	15	1.7
CH_4 (N_2+1.2% H_2O)*	6057.09	760	$3.7 \cdot 10^{-9}$	16	0.24
CO_2 (breath ~50% RH)	6361.25	150	$8.2 \cdot 10^{-9}$	45	40
H_2S (N_2)*	6357.63	780	$5.6 \cdot 10^{-9}$	45	5
HCl (N_2 dry)	5739.26	760	$5.2 \cdot 10^{-8}$	15	0.7
CO_2 (N_2+1.5% H2O) *	4991.26	50	$1.4 \cdot 10^{-8}$	4.4	18
CH_2O (N_2: 75% RH)*	2804.90	75	$8.7 \cdot 10^{-9}$	7.2	0.12
CO (N_2 +2.2% H_2O)	2176.28	100	$1.4 \cdot 10^{-7}$	71	0.002
CO (propylene)	2196.66	50	$7.4 \cdot 10^{-8}$	6.5	0.14
N_2O (air+5%SF_6)	2195.63	50	$1.5 \cdot 10^{-8}$	19	0.007
NO (N_2+H_2O)	1900.07	250	$7.5 \cdot 10^{-9}$	100	0.003
C_2H_5OH (N_2)**	1934.2	770	$2.2 \cdot 10^{-7}$	10	90
C_2HF_5 (N_2)***	1208.62	770	$7.8 \cdot 10^{-9}$	6.6	0.009
NH_3 (N_2)*	1046.39	110	$1.6 \cdot 10^{-8}$	20	0.006

* - Improved microresonator
** - Improved microresonator and double optical pass through ADM
*** - With amplitude modulation and metal microresonator

NNEA – normalized noise equivalent absorption coefficient
NEC – noise equivalent concentration for available laser power and τ=1s time constant, 18 dB/oct filter slope

For comparison: conventional PAS 2.2 (2.6)$\cdot 10^{-9}$ $cm^{-1}W/Hz^{1/2}$ (1,000; 10,000 Hz) for NH_3*

* M. E. Webber et al, Appl. Opt. 42, 2119-2126 (2003); ** J. S. Pilgrim et al. SAE Intl ICES 2007-01-3152

36

Recent Applications of Mid-Infrared Quantum Cascade Laser based QEPAS Sensors to Environmental Monitoring

The global carbon cycle

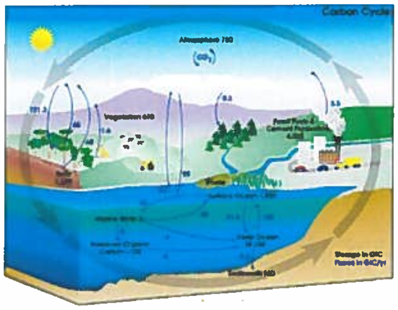

Carbon Dioxide Emissions

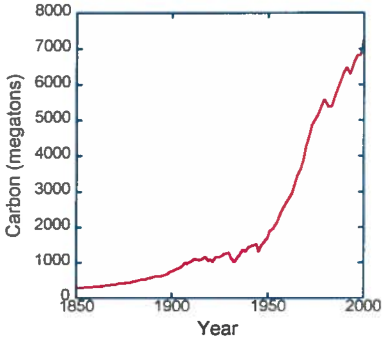

Atmospheric CO_2 Concentration

Last Glacial Maximum to present

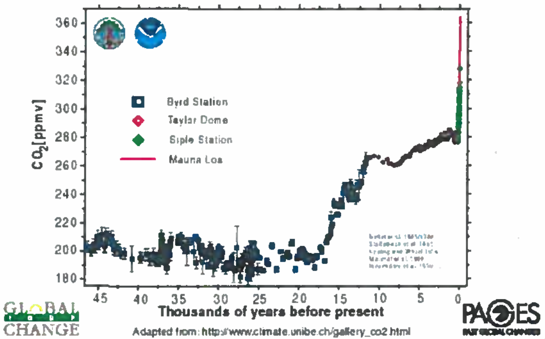

Adapted from: http://www.climate.unibe.ch/gallery_co2.html

T rise for different CO_2 emissions & Models

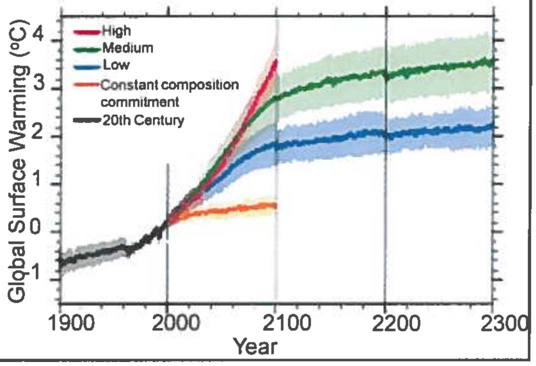

Motivation for NH_3 Detection

- Monitoring of gas separation processes
- Detection of ammonium-nitrate explosives
- Spacecraft related gas monitoring
- Monitoring NH_3 concentrations in the exhaust stream of NO_x removal systems based on selective catalytic reduction (SCR) techniques
- Semiconductor process monitoring & control
- Monitoring of industrial refrigeration facilities
- Pollutant gas monitoring
- Atmospheric chemistry
- Medical diagnostics (kidney & liver diseases)

RICE

42

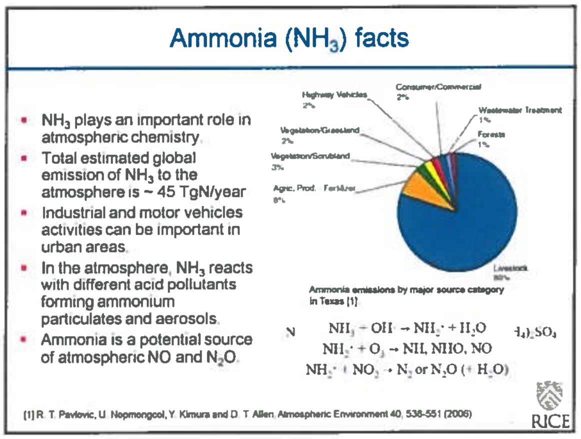

Ammonia (NH_3) facts

- NH_3 plays an important role in atmospheric chemistry.
- Total estimated global emission of NH_3 to the atmosphere is ~ 45 TgN/year
- Industrial and motor vehicles activities can be important in urban areas.
- In the atmosphere, NH_3 reacts with different acid pollutants forming ammonium particulates and aerosols.
- Ammonia is a potential source of atmospheric NO and N_2O.

Ammonia emissions by major source category in Texas [1]

N $NH_3 + OH \rightarrow NH_2\cdot + H_2O$ $_4)_2SO_4$

$NH_2\cdot + O_3 \rightarrow NH, NHO, NO$

$NH_2\cdot + NO_2 \rightarrow N_2 \text{ or } N_2O\ (+ H_2O)$

[1] R. T. Pavlovic, U. Nopmongcol, Y. Kimura and D. T. Allen, Atmospheric Environment 40, 538-551 (2006)

RICE

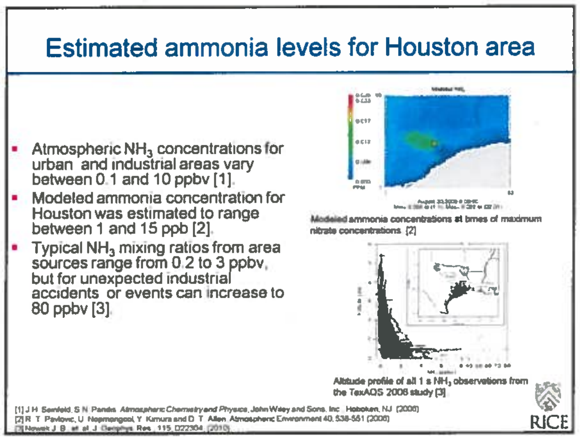

Estimated ammonia levels for Houston area

- Atmospheric NH_3 concentrations for urban and industrial areas vary between 0.1 and 10 ppbv [1].
- Modeled ammonia concentration for Houston was estimated to range between 1 and 15 ppb [2].
- Typical NH_3 mixing ratios from area sources range from 0.2 to 3 ppbv, but for unexpected industrial accidents or events can increase to 80 ppbv [3].

Modeled ammonia concentrations at times of maximum nitrate concentrations [2]

Altitude profile of all 1 s NH_3 observations from the TexAQS 2006 study [3]

[1] J. H. Seinfeld, S. N. Pandis, *Atmospheric Chemistry and Physics*, John Wiley and Sons, Inc., Hoboken, NJ (2006)
[2] R. T. Pavlovic, U. Nopmongcol, Y. Kimura and D. T. Allen, Atmospheric Environment 40, 538-551 (2006)
[3] Nowak J. B. et al. J. Geophys. Res., 115, D22304 (2010)

RICE

l

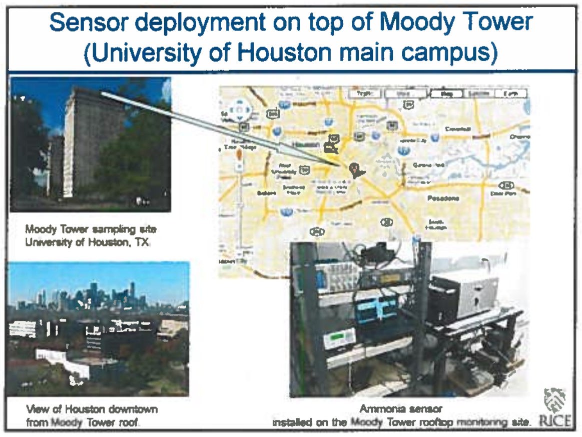

Sensor deployment on top of Moody Tower (University of Houston main campus)

Moody Tower sampling site
University of Houston, TX.

View of Houston downtown
from Moody Tower roof.

Ammonia sensor
installed on the Moody Tower rooftop monitoring site.

RICE

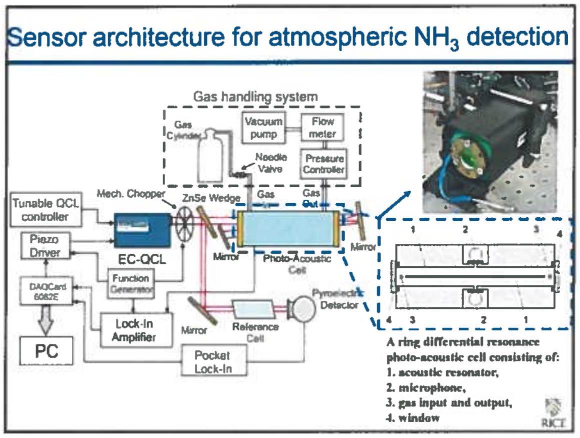

Sensor architecture for atmospheric NH_3 detection

A ring differential resonance photo-acoustic cell consisting of:
1. acoustic resonator,
2. microphone,
3. gas input and output,
4. window

RICE

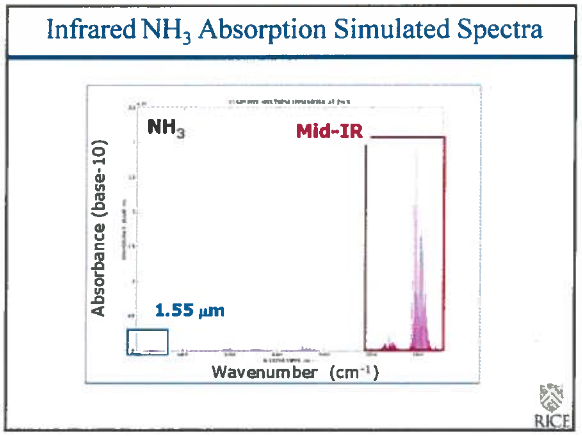

Infrared NH_3 Absorption Simulated Spectra

RICE

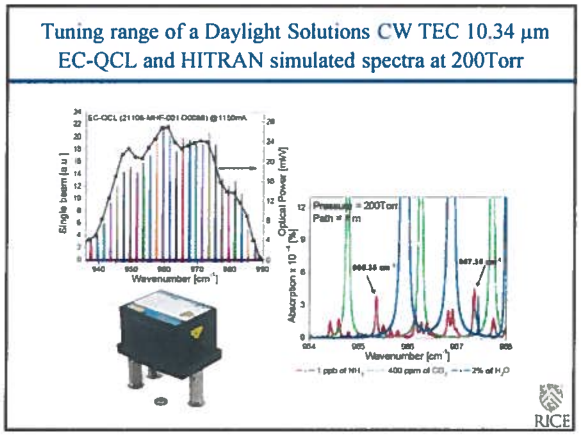

Tuning range of a Daylight Solutions CW TEC 10.34 μm EC-QCL and HITRAN simulated spectra at 200Torr

RICE

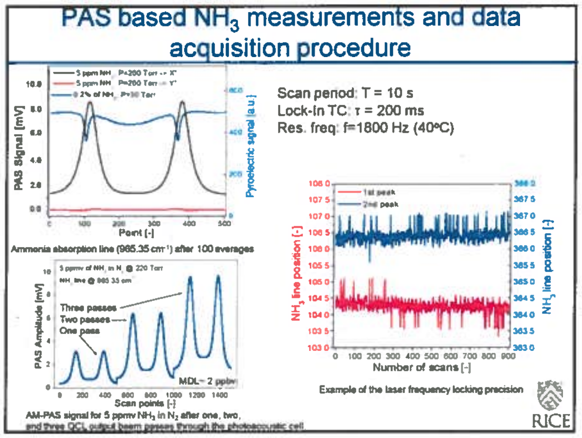

PAS based NH_3 measurements and data acquisition procedure

Scan period: T = 10 s
Lock-In TC: τ = 200 ms
Res. freq: f=1800 Hz (40°C)

Ammonia absorption line (965.35 cm^{-1}) after 100 averages

AM-PAS signal for 5 ppmv NH_3 in N_2 after one, two, and three QCL output beam passes through the photoacoustic cell

Example of the laser frequency locking precision

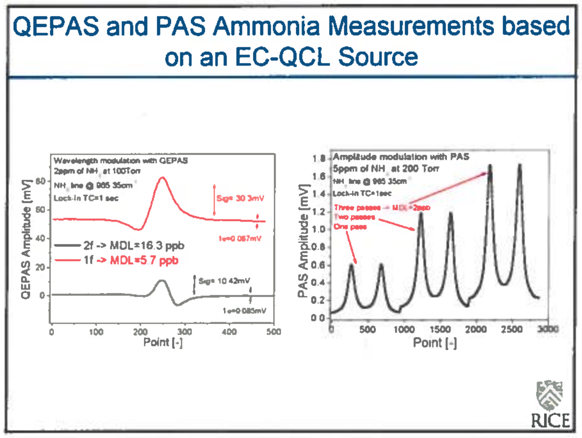

QEPAS and PAS Ammonia Measurements based on an EC-QCL Source

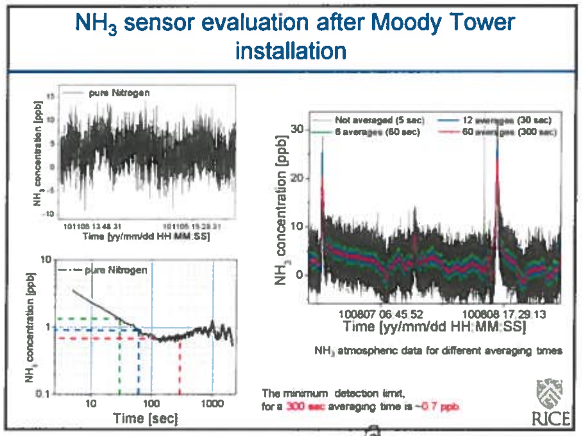

NH_3 sensor evaluation after Moody Tower installation

NH_3 atmospheric data for different averaging times

The minimum detection limit, for a 300 sec averaging time is ~0.7 ppb

2

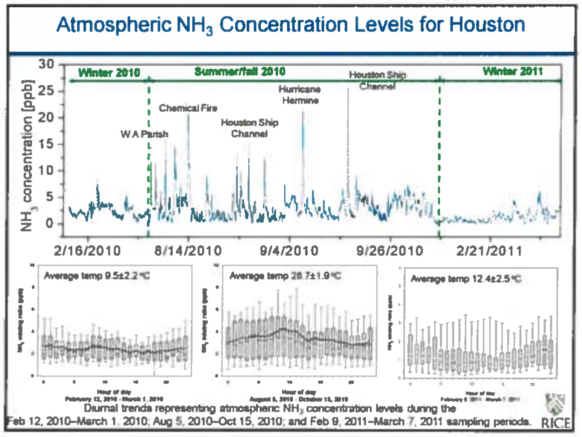

Atmospheric NH_3 Concentration Levels for Houston

Diurnal trends representing atmospheric NH_3 concentration levels during the Feb 12, 2010–March 1, 2010; Aug 5, 2010–Oct 15, 2010; and Feb 9, 2011–March 7, 2011 sampling periods.

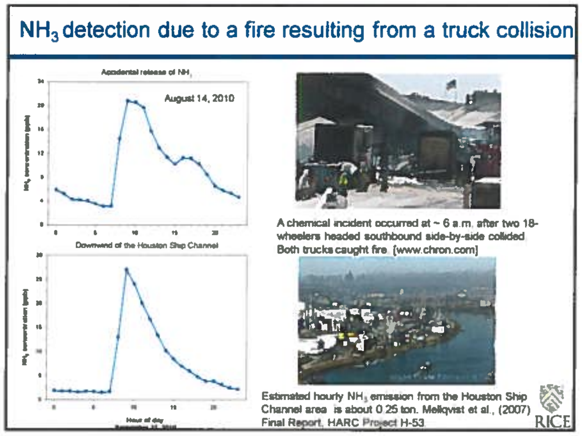

NH_3 detection due to a fire resulting from a truck collision

A chemical incident occurred at ~ 6 a.m. after two 18-wheelers headed southbound side-by-side collided. Both trucks caught fire. [www.chron.com]

Estimated hourly NH_3 emission from the Houston Ship Channel area is about 0.25 ton. Mellqvist et al., (2007) Final Report, HARC Project H-53

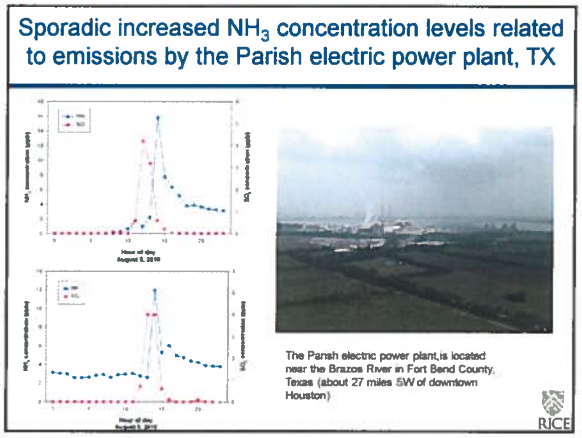

Sporadic increased NH_3 concentration levels related to emissions by the Parish electric power plant, TX

The Parish electric power plant,is located near the Brazos River in Fort Bend County, Texas (about 27 miles SW of downtown Houston)

54

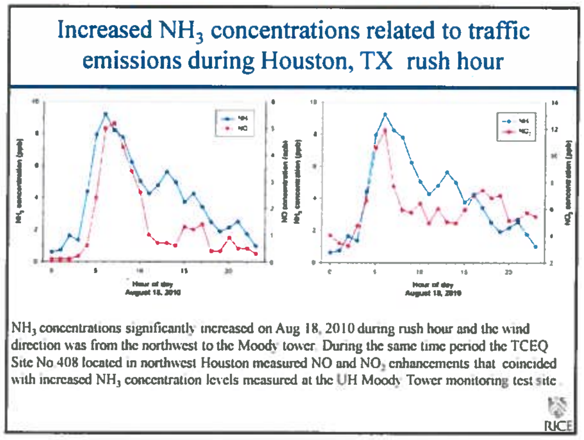

Increased NH_3 concentrations related to traffic emissions during Houston, TX rush hour

NH_3 concentrations significantly increased on Aug 18, 2010 during rush hour and the wind direction was from the northwest to the Moody tower. During the same time period the TCEQ Site No 408 located in northwest Houston measured NO and NO_2 enhancements that coincided with increased NH_3 concentration levels measured at the UH Moody Tower monitoring test site.

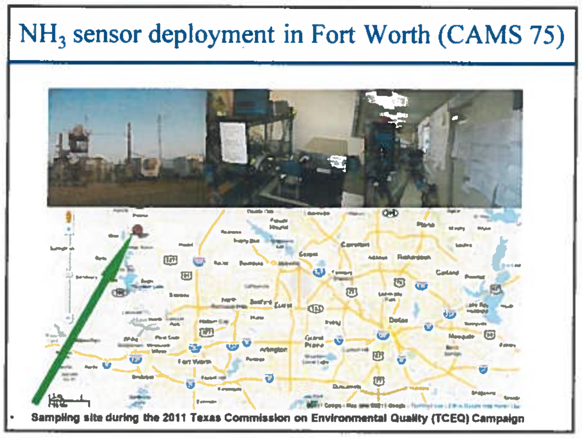

NH_3 sensor deployment in Fort Worth (CAMS 75)

- Sampling site during the 2011 Texas Commission on Environmental Quality (TCEQ) Campaign

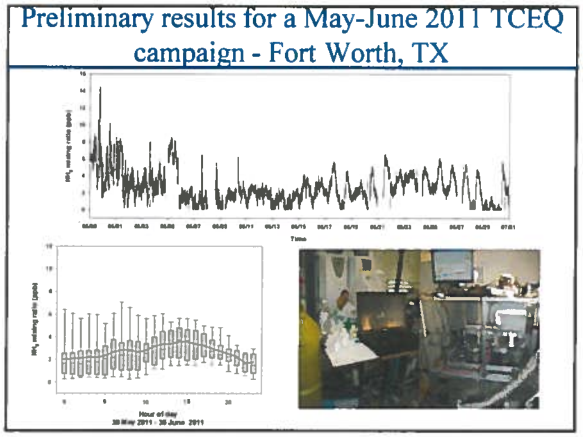

Preliminary results for a May-June 2011 TCEQ campaign - Fort Worth, TX

Recent Applications of Mid-Infrared Quantum Cascade Laser based QEPAS Sensors to Breath Analysis

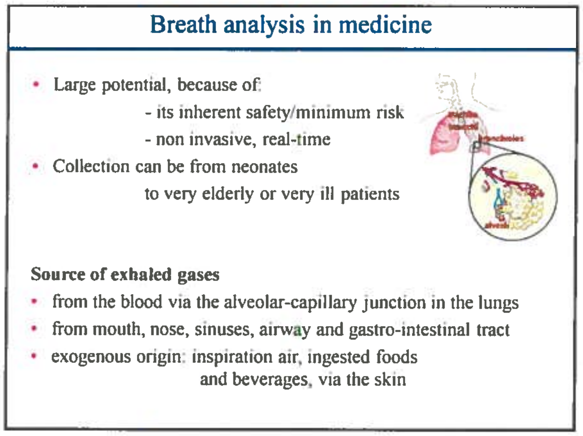

Breath analysis in medicine

- Large potential, because of:
  - its inherent safety/minimum risk
  - non invasive, real-time
- Collection can be from neonates to very elderly or very ill patients

Source of exhaled gases

- from the blood via the alveolar-capillary junction in the lungs
- from mouth, nose, sinuses, airway and gastro-intestinal tract
- exogenous origin: inspiration air, ingested foods and beverages, via the skin

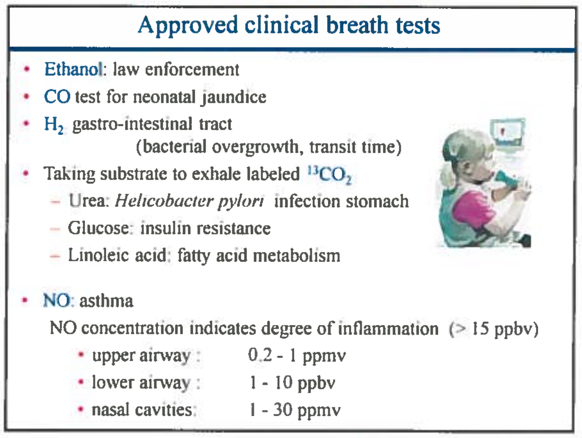

Approved clinical breath tests

- Ethanol: law enforcement
- CO test for neonatal jaundice
- H_2 gastro-intestinal tract (bacterial overgrowth, transit time)
- Taking substrate to exhale labeled $^{13}CO_2$
  - Urea: *Helicobacter pylori* infection stomach
  - Glucose: insulin resistance
  - Linoleic acid: fatty acid metabolism
- NO: asthma

NO concentration indicates degree of inflammation (> 15 ppbv)

- upper airway : 0.2 - 1 ppmv
- lower airway : 1 - 10 ppbv
- nasal cavities: 1 - 30 ppmv

60

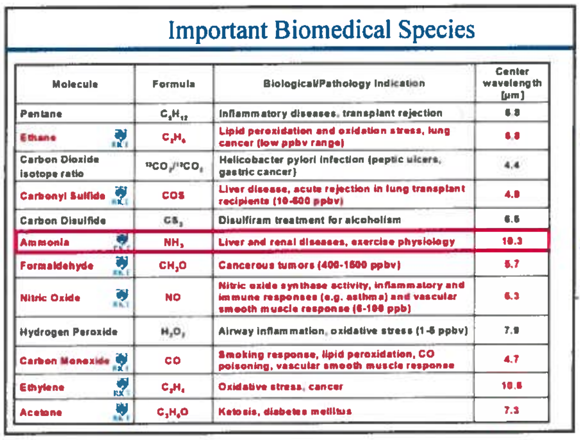

Important Biomedical Species

Molecule	Formula	Biological/Pathology Indication	Center wavelength [µm]
Pentane	C_5H_{12}	Inflammatory diseases, transplant rejection	6.8
Ethane	C_2H_6	Lipid peroxidation and oxidation stress, lung cancer (low ppbv range)	6.8
Carbon Dioxide isotope ratio	$^{13}CO_2/^{12}CO_2$	Helicobacter pylori infection (peptic ulcers, gastric cancer)	4.4
Carbonyl Sulfide	COS	Liver disease, acute rejection in lung transplant recipients (10-600 ppbv)	4.9
Carbon Disulfide	CS_2	Disulfiram treatment for alcoholism	6.5
Ammonia	NH_3	Liver and renal diseases, exercise physiology	10.3
Formaldehyde	CH_2O	Cancerous tumors (400-1600 ppbv)	5.7
Nitric Oxide	NO	Nitric oxide synthase activity, inflammatory and immune responses (e.g. asthma) and vascular smooth muscle response (6-100 ppb)	5.3
Hydrogen Peroxide	H_2O_2	Airway inflammation, oxidative stress (1-5 ppbv)	7.8
Carbon Monoxide	CO	Smoking response, lipid peroxidation, CO poisoning, vascular smooth muscle response	4.7
Ethylene	C_2H_4	Oxidative stress, cancer	10.6
Acetone	C_3H_6O	Ketosis, diabetes mellitus	7.3

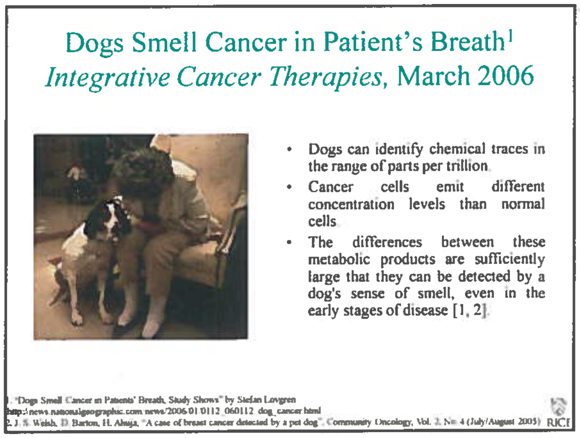

Dogs Smell Cancer in Patient's Breath[1]
Integrative Cancer Therapies, March 2006

- Dogs can identify chemical traces in the range of parts per trillion
- Cancer cells emit different concentration levels than normal cells
- The differences between these metabolic products are sufficiently large that they can be detected by a dog's sense of smell, even in the early stages of disease [1, 2]

[1] "Dogs Smell Cancer in Patients' Breath, Study Shows" by Stefan Lovgren http://news.nationalgeographic.com/news/2006/01/0112_060112_dog_cancer.html

[2] J. S. Welsh, D. Barton, H. Ahuja, "A case of breast cancer detected by a pet dog", Community Oncology, Vol. 2, No 4 (July/August 2005)

RICE

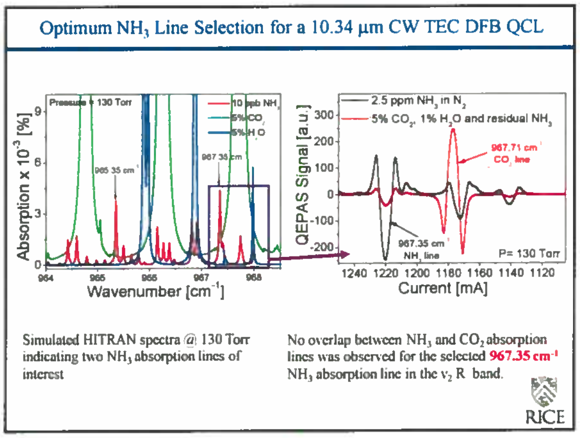

Optimum NH_3 Line Selection for a 10.34 µm CW TEC DFB QCL

Simulated HITRAN spectra @ 130 Torr indicating two NH_3 absorption lines of interest

No overlap between NH_3 and CO_2 absorption lines was observed for the selected **967.35 cm^{-1}** NH_3 absorption line in the v_2 R band.

RICE

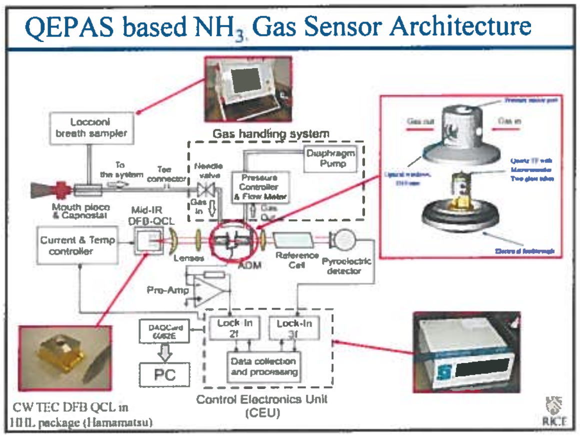

QEPAS based NH_3 Gas Sensor Architecture

CW TEC DFB QCL in HHL package (Hamamatsu)

RICE

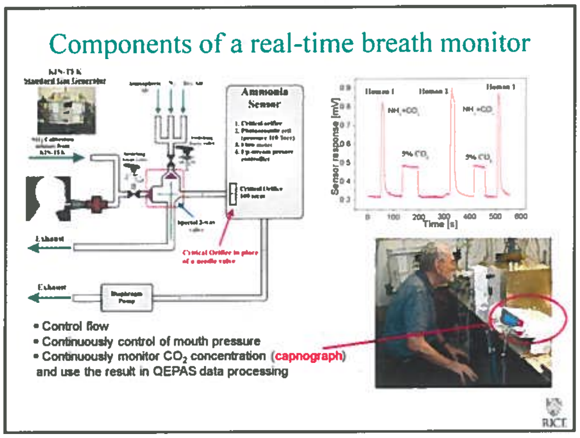

Components of a real-time breath monitor

- Control flow
- Continuously control of mouth pressure
- Continuously monitor CO_2 concentration (capnograph) and use the result in QEPAS data processing

RICE

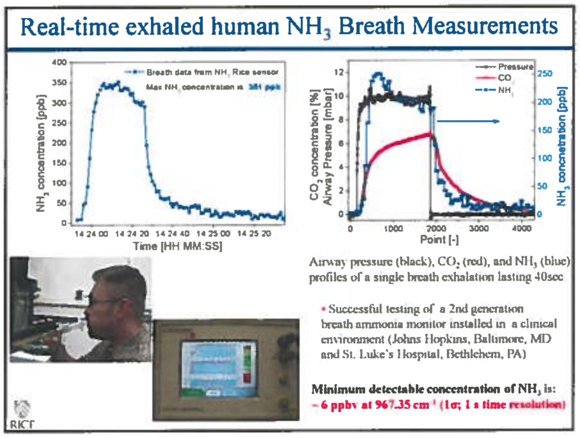

Real-time exhaled human NH_3 Breath Measurements

Airway pressure (black), CO_2 (red), and NH_3 (blue) profiles of a single breath exhalation lasting 40sec

- Successful testing of a 2nd generation breath ammonia monitor installed in a clinical environment (Johns Hopkins, Baltimore, MD and St. Luke's Hospital, Bethlehem, PA)

Minimum detectable concentration of NH_3 is:
~6 ppbv at 967.35 cm^{-1} (1σ; 1 s time resolution)

RICE

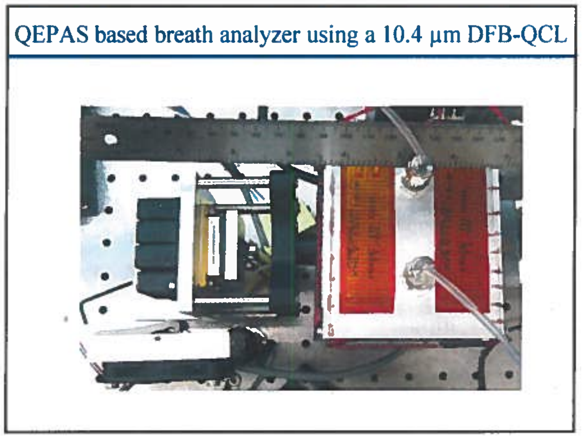

QEPAS based breath analyzer using a 10.4 µm DFB-QCL

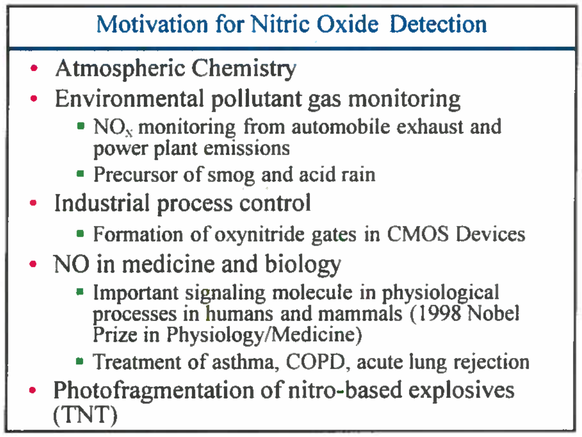

Motivation for Nitric Oxide Detection

- Atmospheric Chemistry
- Environmental pollutant gas monitoring
  - NO_x monitoring from automobile exhaust and power plant emissions
  - Precursor of smog and acid rain
- Industrial process control
  - Formation of oxynitride gates in CMOS Devices
- NO in medicine and biology
  - Important signaling molecule in physiological processes in humans and mammals (1998 Nobel Prize in Physiology/Medicine)
  - Treatment of asthma, COPD, acute lung rejection
- Photofragmentation of nitro-based explosives (TNT)

12

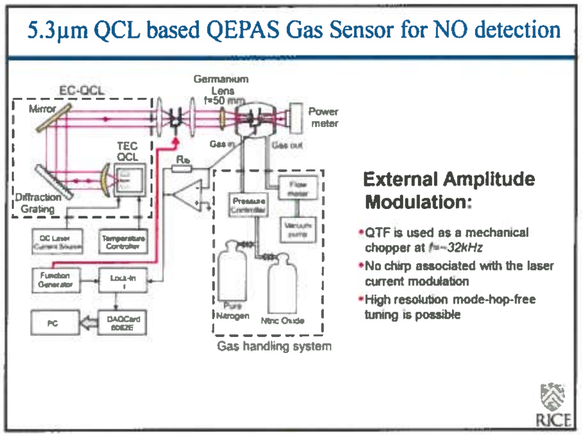

5.3µm QCL based QEPAS Gas Sensor for NO detection

External Amplitude Modulation:

- QTF is used as a mechanical chopper at *f=~32kHz*
- No chirp associated with the laser current modulation
- High resolution mode-hop-free tuning is possible

2

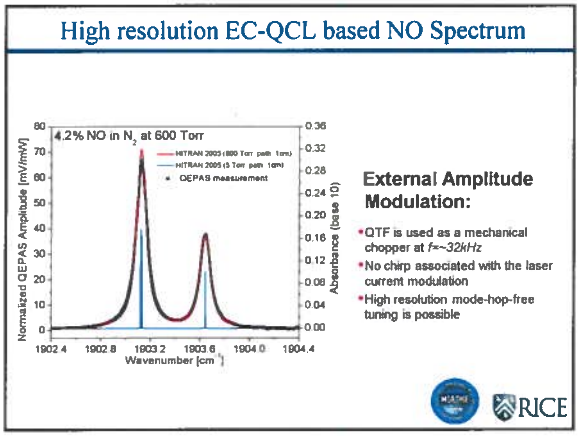

High resolution EC-QCL based NO Spectrum

External Amplitude Modulation:

- QTF is used as a mechanical chopper at *f=~32kHz*
- No chirp associated with the laser current modulation
- High resolution mode-hop-free tuning is possible

2

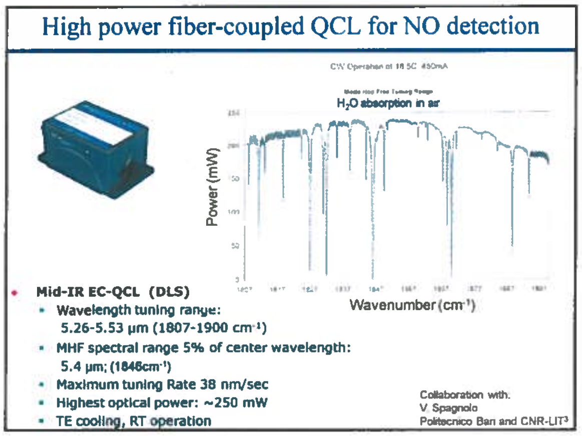

High power fiber-coupled QCL for NO detection

- **Mid-IR EC-QCL (DLS)**
  - Wavelength tuning range: 5.26-5.53 µm (1807-1900 cm⁻¹)
  - MHF spectral range 5% of center wavelength: 5.4 µm; (1846cm⁻¹)
  - Maximum tuning Rate 38 nm/sec
  - Highest optical power: ~250 mW
  - TE cooling, RT operation

Collaboration with:
V. Spagnolo
Politecnico Bari and CNR-LIT³

2

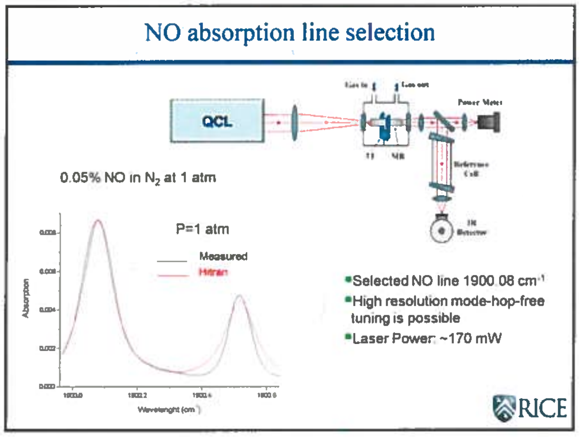

NO absorption line selection

- Selected NO line 1900.08 cm⁻¹
- High resolution mode-hop-free tuning is possible
- Laser Power: ~170 mW

2

72

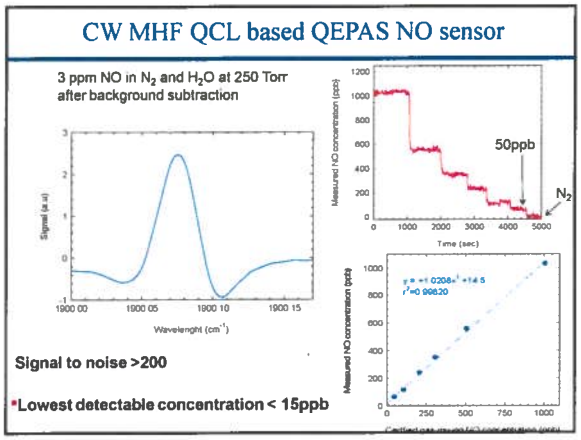

CW MHF QCL based QEPAS NO sensor

3 ppm NO in N_2 and H_2O at 250 Torr after background subtraction

Signal to noise >200

- Lowest detectable concentration < 15ppb

2

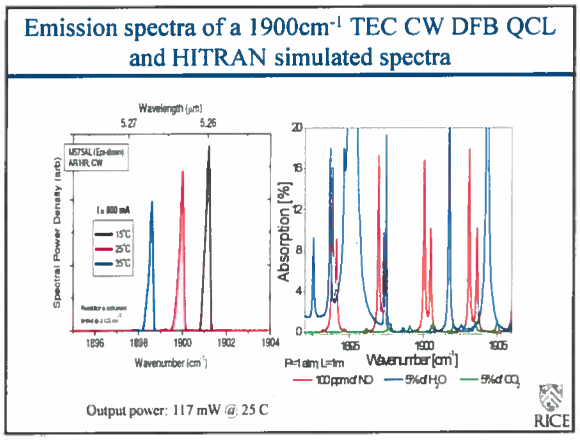

Emission spectra of a 1900cm⁻¹ TEC CW DFB QCL and HITRAN simulated spectra

Output power: 117 mW @ 25 C

2

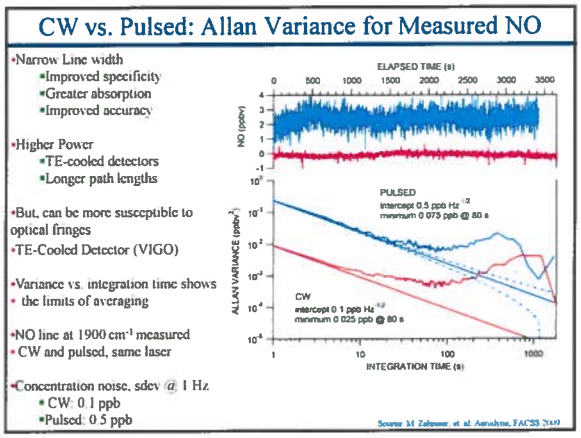

CW vs. Pulsed: Allan Variance for Measured NO

- Narrow Line width
  - Improved specificity
  - Greater absorption
  - Improved accuracy
- Higher Power
  - TE-cooled detectors
  - Longer path lengths
- But, can be more susceptible to optical fringes
- TE-Cooled Detector (VIGO)
- Variance vs. integration time shows
- the limits of averaging
- NO line at 1900 cm⁻¹ measured
- CW and pulsed, same laser
- Concentration noise, sdev @ 1 Hz
  - CW: 0.1 ppb
  - Pulsed: 0.5 ppb

Source: M. Zahniser, et al. Aerodyne, FACSS 2009

2

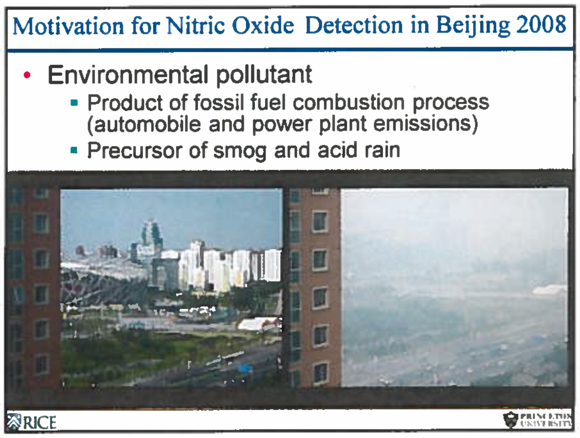

Motivation for Nitric Oxide Detection in Beijing 2008

- Environmental pollutant
  - Product of fossil fuel combustion process (automobile and power plant emissions)
  - Precursor of smog and acid rain

2

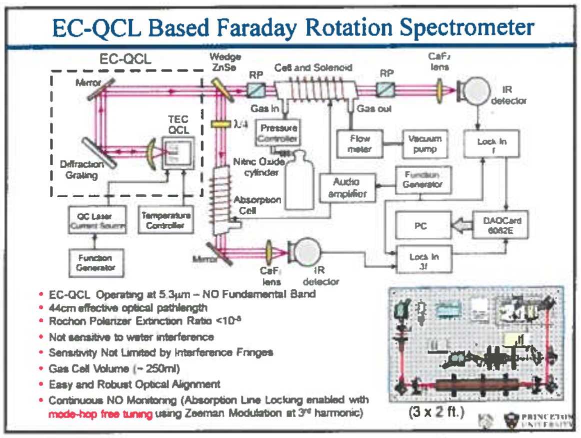

EC-QCL Based Faraday Rotation Spectrometer

- EC-QCL Operating at 5.3µm – NO Fundamental Band
- 44cm effective optical pathlength
- Rochon Polarizer Extinction Ratio <10⁻⁵
- Not sensitive to water interference
- Sensitivity Not Limited by Interference Fringes
- Gas Cell Volume (~ 250ml)
- Easy and Robust Optical Alignment
- Continuous NO Monitoring (Absorption Line Locking enabled with mode-hop free tuning using Zeeman Modulation at 3rd harmonic)

(3 x 2 ft.)

2

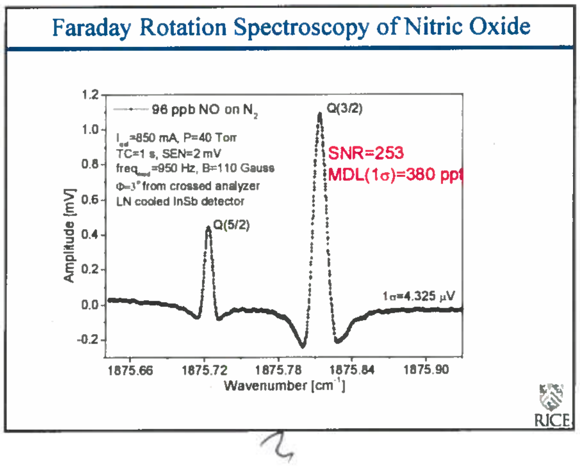

Faraday Rotation Spectroscopy of Nitric Oxide

2

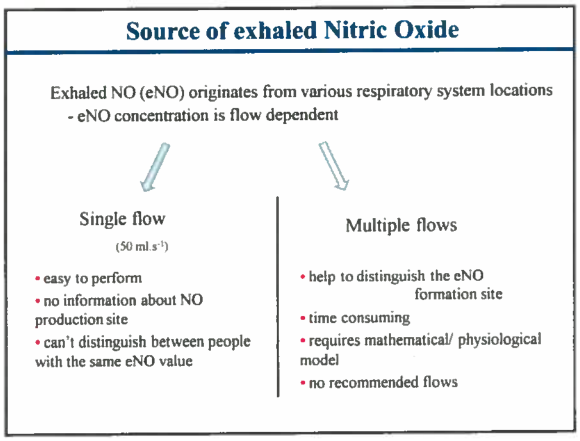

Source of exhaled Nitric Oxide

Exhaled NO (eNO) originates from various respiratory system locations
- eNO concentration is flow dependent

Single flow

(50 ml s⁻¹)

- easy to perform
- no information about NO production site
- can't distinguish between people with the same eNO value

Multiple flows

- help to distinguish the eNO formation site
- time consuming
- requires mathematical/ physiological model
- no recommended flows

2

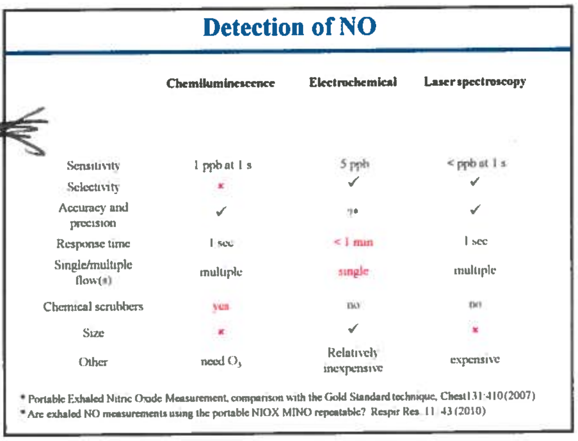

Detection of NO

	Chemiluminescence	Electrochemical	Laser spectroscopy
Sensitivity	1 ppb at 1 s	5 ppb	< ppb at 1 s
Selectivity	✗	✓	✓
Accuracy and precision	✓	?*	✓
Response time	1 sec	< 1 min	1 sec
Single/multiple flow(s)	multiple	single	multiple
Chemical scrubbers	yes	no	no
Size	✗	✓	✗
Other	need O_3	Relatively inexpensive	expensive

* Portable Exhaled Nitric Oxide Measurement, comparison with the Gold Standard technique, Chest131:410(2007)
* Are exhaled NO measurements using the portable NIOX MINO repeatable? Respir Res. 11 43 (2010)

2

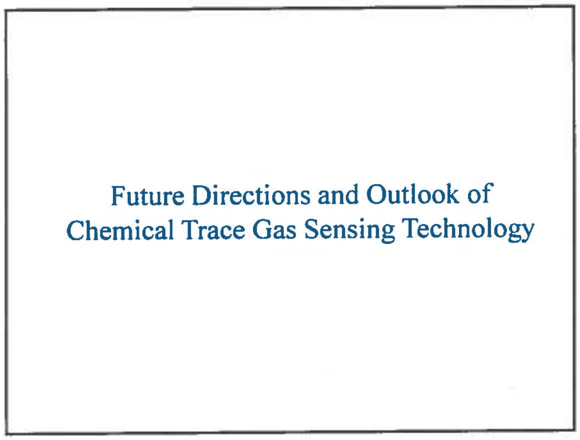

Future Directions and Outlook of Chemical Trace Gas Sensing Technology

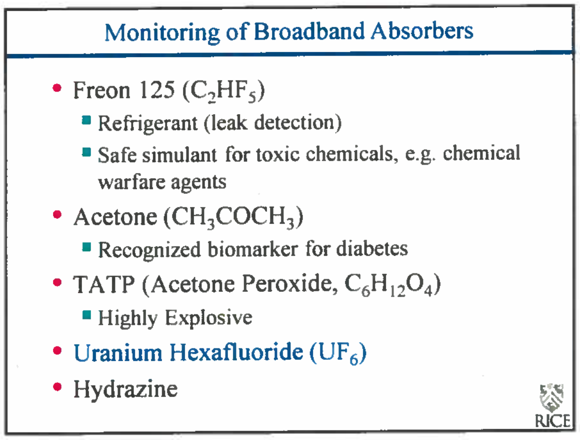

Monitoring of Broadband Absorbers

- Freon 125 (C_2HF_5)
  - Refrigerant (leak detection)
  - Safe simulant for toxic chemicals, e.g. chemical warfare agents
- Acetone (CH_3COCH_3)
  - Recognized biomarker for diabetes
- TATP (Acetone Peroxide, $C_6H_{12}O_4$)
  - Highly Explosive
- Uranium Hexafluoride (UF_6)
- Hydrazine

RICE

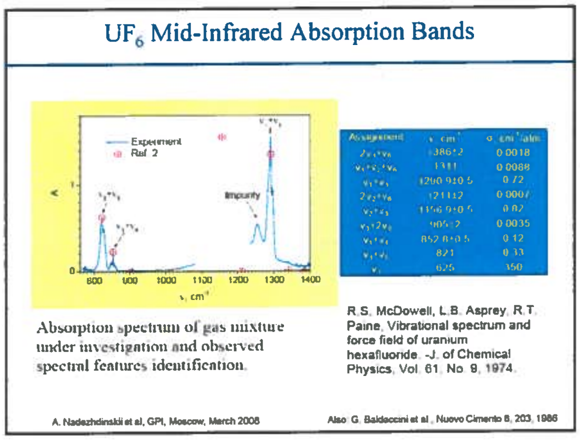

UF_6 Mid-Infrared Absorption Bands

Assignment	ν, cm⁻¹	σ, cm⁻²atm⁻¹
$2\nu_1+\nu_6$	1386±2	0.0018
$\nu_1+\nu_2+\nu_6$	1311	0.0088
$\nu_1+\nu_3$	1290.9±0.5	0.72
$2\nu_2+\nu_6$	1211±2	0.0007
$\nu_2+\nu_3$	1156.9±0.5	0.02
$\nu_3+2\nu_6$	905±2	0.0035
$\nu_3+\nu_4$	852.8±0.5	0.12
$\nu_3+\nu_6$	821	0.33
ν_3	625	350

Absorption spectrum of gas mixture under investigation and observed spectral features identification.

R.S. McDowell, L.B. Asprey, R.T. Paine, Vibrational spectrum and force field of uranium hexafluoride. -J. of Chemical Physics, Vol. 61, No. 9, 1974.

A. Nadezhdinskii et al, GPI, Moscow, March 2008

Also: G. Baldacci et al., Nuovo Cimento 8, 203, 1986

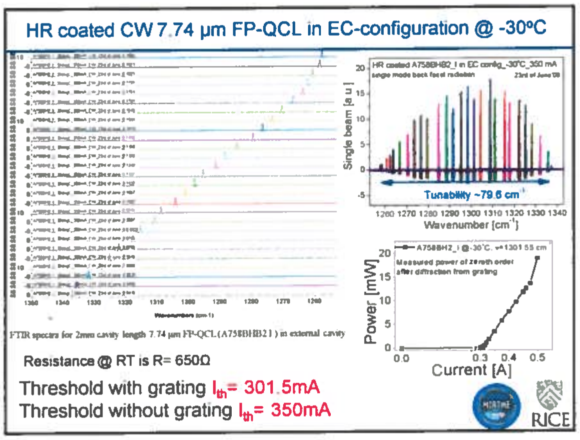

HR coated CW 7.74 µm FP-QCL in EC-configuration @ -30°C

FTIR specra for 2mm cavity length 7.74 µm FP-QCL (A758BHB2 1) in external cavity

Resistance @ RT is R= 650Ω

Threshold with grating I_{th}= 301.5mA

Threshold without grating I_{th}= 350mA

RICE

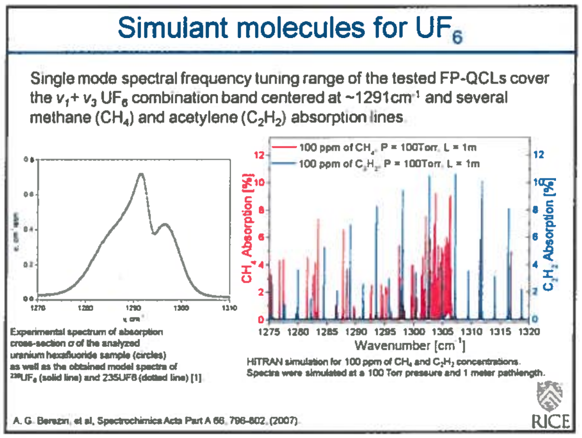

Simulant molecules for UF_6

Single mode spectral frequency tuning range of the tested FP-QCLs cover the $\nu_1 + \nu_3$ UF_6 combination band centered at ~1291cm⁻¹ and several methane (CH_4) and acetylene (C_2H_2) absorption lines

Experimental spectrum of absorption cross-section σ of the analyzed uranium hexafluoride sample (circles) as well as the obtained model spectra of $^{238}UF_6$ (solid line) and 235UF6 (dotted line) [1]

HITRAN simulation for 100 ppm of CH_4 and C_2H_2 concentrations. Spectra were simulated at a 100 Torr pressure and 1 meter pathlength.

A. G. Berezin, et al, Spectrochimica Acta Part A 66, 796-802, (2007)

RICE

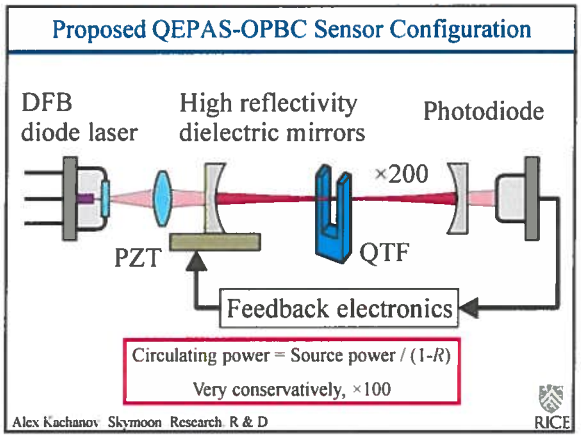

Proposed QEPAS-OPBC Sensor Configuration

Circulating power = Source power / (1-*R*)

Very conservatively, ×100

Alex Kachanov, Skymoon Research R & D

RICE

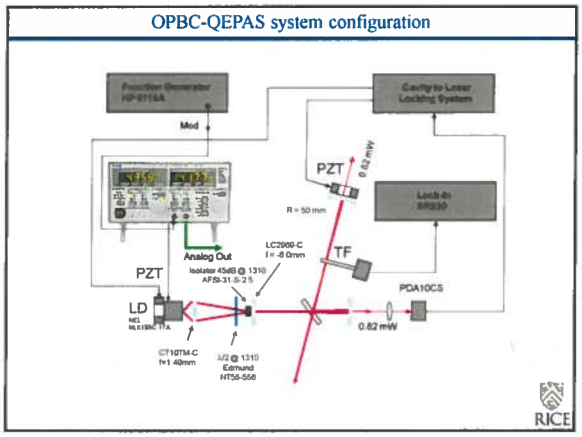

OPBC-QEPAS system configuration

RICE

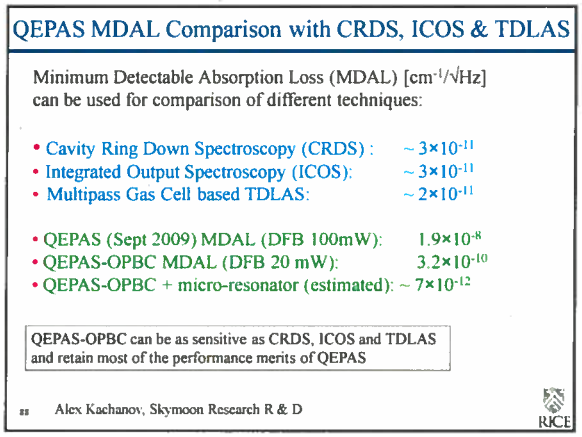

QEPAS MDAL Comparison with CRDS, ICOS & TDLAS

Minimum Detectable Absorption Loss (MDAL) [cm⁻¹/√Hz] can be used for comparison of different techniques:

- Cavity Ring Down Spectroscopy (CRDS) : ~ 3×10^{-11}
- Integrated Output Spectroscopy (ICOS): ~ 3×10^{-11}
- Multipass Gas Cell based TDLAS: ~ 2×10^{-11}

- QEPAS (Sept 2009) MDAL (DFB 100mW): 1.9×10^{-8}
- QEPAS-OPBC MDAL (DFB 20 mW): 3.2×10^{-10}
- QEPAS-OPBC + micro-resonator (estimated): ~ 7×10^{-12}

QEPAS-OPBC can be as sensitive as CRDS, ICOS and TDLAS and retain most of the performance merits of QEPAS

Alex Kachanov, Skymoon Research R & D

RICE

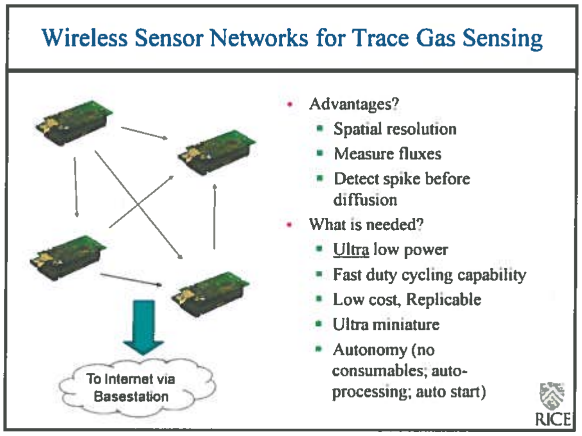

Wireless Sensor Networks for Trace Gas Sensing

- Advantages?
  - Spatial resolution
  - Measure fluxes
  - Detect spike before diffusion
- What is needed?
  - Ultra low power
  - Fast duty cycling capability
  - Low cost, Replicable
  - Ultra miniature
  - Autonomy (no consumables; auto-processing; auto start)

RICE

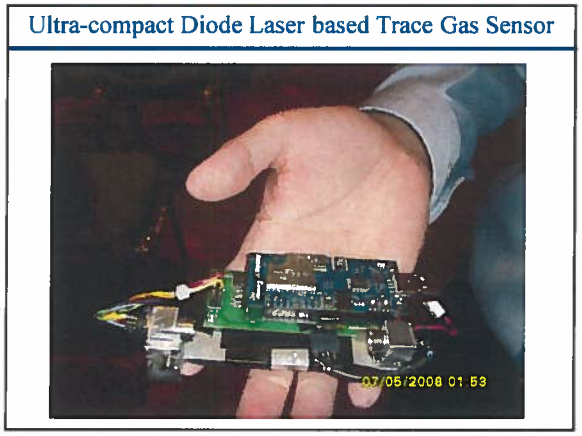

Ultra-compact Diode Laser based Trace Gas Sensor

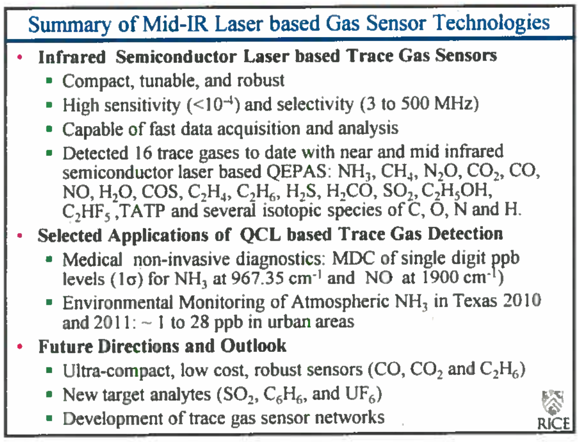

Summary of Mid-IR Laser based Gas Sensor Technologies

- **Infrared Semiconductor Laser based Trace Gas Sensors**
  - Compact, tunable, and robust
  - High sensitivity ($<10^{-4}$) and selectivity (3 to 500 MHz)
  - Capable of fast data acquisition and analysis
  - Detected 16 trace gases to date with near and mid infrared semiconductor laser based QEPAS: NH_3, CH_4, N_2O, CO_2, CO, NO, H_2O, COS, C_2H_4, C_2H_6, H_2S, H_2CO, SO_2, C_2H_5OH, C_2HF_5 ,TATP and several isotopic species of C, O, N and H.
- **Selected Applications of QCL based Trace Gas Detection**
  - Medical non-invasive diagnostics: MDC of single digit ppb levels (1σ) for NH_3 at 967.35 cm^{-1} and NO at 1900 cm^{-1})
  - Environmental Monitoring of Atmospheric NH_3 in Texas 2010 and 2011: ~ 1 to 28 ppb in urban areas
- **Future Directions and Outlook**
  - Ultra-compact, low cost, robust sensors (CO, CO_2 and C_2H_6)
  - New target analytes (SO_2, C_6H_6, and UF_6)
  - Development of trace gas sensor networks

RICE